

Electronic and Magnetic Properties of Ultrathin Fe–Co Alloy Nanowires

Chulsu Jo,^{*,†} Jae Il Lee,^{†,§} and Youngrok Jang^{‡,||}

Department of Physics, Inha University, Incheon 402-751, Korea, and Department of Physics, University of Incheon, Incheon 402-749, Korea

Received November 30, 2004. Revised Manuscript Received January 30, 2005

We have investigated the electronic structures and magnetic properties of free-standing Fe–Co nanowires by density functional theory (DFT) calculations using ultrasoft pseudopotential plane wave method. We have considered the free-standing $\text{Fe}_{(1-x)}\text{Co}_x$ nanowires with centered-staggered triangle and square structures. The optimized lattice constants obtained by total energy calculation are slightly longer than those of the experimental results and the variation of magnetic moments with Co concentration is similar to the Slater–Pauling curve. The spin-polarized density of states (DOS) of $\text{Fe}_{0.8}\text{Co}_{0.2}$ nanowire reveals a nearly half-metallic character. We have found the coercivity estimated by the chain-of-spheres model is consistent with the experimental results for Fe–Co nanowire arrays fabricated in porous templates.

Introduction

Ferromagnetic nanowires and their arrays are attracting a great deal of interest because of their potential applications in magnetic sensors, memory devices, spintronic nanodevices, and energy storage.^{1–3} They are also good candidates for giant magnetoresistance (GMR) materials without the occurrence of structural defects in multilayers. The magnetic nanowire arrays have high-density recording ability in excess of 100 Gb/in.². In particular, Fe-rich nanowire alloys with high coercivity are widely used to control the magnetic properties of recording media by varying the concentration.⁴

The parallel $\text{Fe}_{(1-x)}\text{Co}_x$ nanowire arrays were synthesized along the step edges on a W(110) substrate.⁵ The Curie temperature of these nanowire arrays rapidly decreases at $x = 0.35$ and a ferromagnetic easy axis exists below $x = 0.35$. In general, highly ordered Fe–Co nanowire arrays are produced by electrodeposition into porous templates.^{4–7} The magnetic properties usually vary with the nanowire diameter, length, and interwire distance, which are easily controlled by electrochemical parameters. Qin et al. have observed that the coercivity and squareness ratio (M_r/M_s , where M_r and M_s indicate remanent and spontaneous magnetization, re-

spectively) of $\text{Fe}_{(1-x)}\text{Co}_x$ nanowires within nanopores have peak around $x = 0.8$ and decrease slowly with decreasing Co concentrations.⁶ For the Co concentrations above $x = 0.9$, the hexagonal close packing (hcp) structures are formed in templates and the coercivity drops down rapidly. When the applied field is perpendicular to the easy axis along the wire length, the coercivity and squareness ratio are much lower than those for the external field parallel to the nanowire arrays. Qin et al. discussed that the results come from the decrease of spontaneous magnetization and anisotropy along nanowire arrays.

The coercivity and squareness ratio are determined by the magnetization reversal process. According to Stoner–Wohlfarth model,⁸ the magnetization of nanowire remains coherent throughout the magnet and their magnetism is mainly influenced by shape anisotropy. In this case, the coercivity is linear with the spontaneous magnetization M_s and is estimated by the magnitude of M_s . Jacobs and Bean proposed the chain-of-spheres model with two reversal mechanisms, i.e., the parallel rotation and symmetric fanning mechanism.⁹ In this model, the nanowire is modeled as a chain of single spheres, which is considered as a single domain without exchange interaction between adjacent spheres. Chen et al. have found the coercivity obtained by the chain-of-spheres model with symmetric fanning mechanisms agreed with the experimental results for Fe–Co nanowires in the nanopores.⁷

On the other hand, many essential characteristics of ferromagnetic Fe–Co nanowire arrays fabricated within templates depend on the pore morphology of templates.¹⁰ Free-standing ferromagnetic nanowires separated from template can be assembled and functionalized. However, it is not easy to separate nanowires from templates and the yield

* To whom correspondence should be addressed. E-mail: goodchul@goodchul.com.

[†] Inha University.

[‡] University of Incheon.

[§] E-mail: jilee@inha.ac.kr.

^{||} E-mail: yrjang@incheon.ac.kr.

- (1) Prinz, G. A. *Science* **1998**, 282, 1660.
- (2) Chou, S. Y.; Wei, M. S.; Krauss, P. R.; Fisher, P. B. *J. Appl. Phys.* **1994**, 76, 6673.
- (3) Guo, Y. G.; Wan, L. J.; Zhu, C. F.; Yang, D. L.; Chen, D. M.; Bai, C. L. *Chem. Mater.* **2003**, 15, 664.
- (4) Zhan, Q.; Chen, Z.; Xue, D.; Li, F.; Kunkel, H.; Zhou, X.; Roshko, R.; Williams, G. *Phys. Rev. B* **2002**, 66, 134436.
- (5) Pierce, J. P.; Plummer, E. W.; Shen, J. *Appl. Phys. Lett.* **2002**, 374, 1890.
- (6) Qin, D. H.; Peng, Y.; Cao, L.; Li, H. L. *Chem. Phys. Lett.* **2003**, 374, 661.
- (7) Chen, W.; Tang, S.; Lu, M.; Du, Y. *J. Phys.: Condens. Matter* **2003**, 15, 4623.

(8) Stoner, E. C.; Wohlfarth, E. P. *Philos. Trans. R. Soc.* **1948**, A240, 599.

(9) Jacobs, I. S.; Bean, C. P. *Phys. Rev.* **1955**, 100, 1060.

(10) Chein, C. L.; Sun, L.; Tanase, M.; Bauer, L. A.; Hultgren, A.; Silevitch, D. M.; Meyer, G. J.; Searson, P. C.; Reich, D. H. *J. Magn. Magn. Mater.* **2002**, 249, 146.

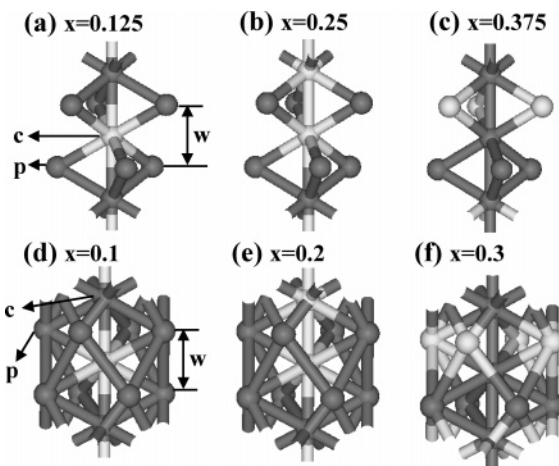


Figure 1. Some $\text{Fe}_{(1-x)}\text{Co}_x$ nanowires with centered-staggered triangle and square structures (black ball for Fe atom and gray ball for Co atom). The “w” denotes wire length along z-axis. The “c” and “p” indicate central atom and planar atom, respectively.

is relatively low. Recently, the free-standing Fe–Co and Fe–Cr nanocluster wire (NCW) bundles were synthesized by a simple fabrication method using a resistive heater placed in the middle of a pair of permanent disk magnets.¹¹ The Fe–Co NCWs have body-centered cubic (bcc) structure below 89 Co mol %.

In this study, we obtained the possible structures of free-standing ultrathin Fe–Co nanowires by DFT calculation. We also calculated the electronic structure, magnetic moment, spin polarization, and coercivity of Fe–Co nanowires. The calculated lattice constants and coercivity are compared with previous experimental results. We showed that free-standing $\text{Fe}_{(1-x)}\text{Co}_x$ nanowire at $x = 0.2$ has high magnetic moment, half-metallic spin polarization, and high coercivity.

Methods

We investigated, using the Vienna Ab Initio Simulation Program (VASP) code,¹² the possible structures and the magnetic properties of free-standing ultrathin Fe–Co nanowires with a variety of Co concentrations. The VASP code is based on DFT using the ultrasoft pseudopotential plane wave method. We considered free-standing $\text{Fe}_{(1-x)}\text{Co}_x$ nanowires with centered-staggered triangle and square structures (Figure 1), which are similar to the stable structures of Fe nanowires.¹³ Spin-polarized calculations are performed in order to obtain magnetic moments and spin polarization. We also calculated the coercivity using the chain-of-spheres model with symmetric fanning mechanism and compared with the experimental values.^{4,6,7} The total energy and electronic structure calculations have been carried out within the generalized gradient approximation (GGA). We used $2 \times 2 \times 10$ k-points meshes in Monkhorst-Pack scheme. The energy cutoff of the plane wave basis set is taken to be 270 eV and the total energies of nanowires are converged to 10^{-3} eV. We optimized geometries until the atomic force is less than 0.01 eV/Å. To check the reasonability of our results, we have been compared the calculated magnetic moment for bcc bulk Fe with experimental values. The calculated magnetic moment for bcc bulk Fe, $2.23 \mu_B/\text{atom}$, is almost the same as that from experiment.¹⁴

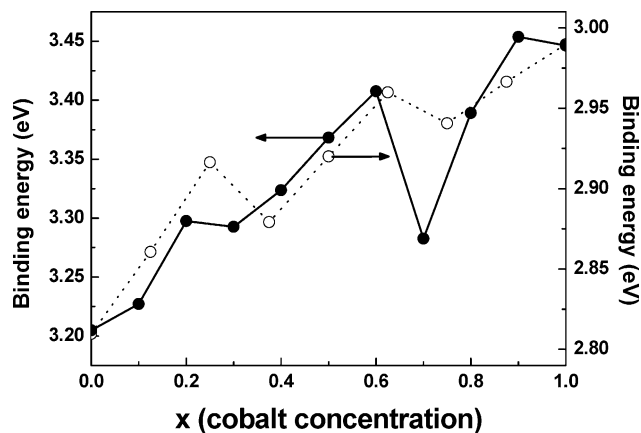


Figure 2. Binding energies of $\text{Fe}_{(1-x)}\text{Co}_x$ nanowires with centered-staggered triangle and square structures. The filled and open circles indicate the Fe–Co nanowires with centered-staggered square and triangle structures, respectively.

The stability of nanowires with Co concentrations is determined from the binding energy (E_b) defined by

$$E_b = (-E_{\text{tot}} + n_{\text{Fe}}E_{\text{Fe}} + n_{\text{Co}}E_{\text{Co}})/(n_{\text{Fe}} + n_{\text{Co}}) \quad (1)$$

where E_{Fe} and E_{Co} are the self-energy of Fe and Co atoms, respectively. The E_{tot} means total energy of Fe–Co nanowire consisting of n_{Fe} and n_{Co} atoms.

Results and Discussion

We show that the binding energies of Fe–Co nanowires with centered-staggered triangle structure are about 0.4 eV lower than those of nanowires with centered-staggered square structure (Figure 2). The binding energies overall increase with increasing Co concentrations. For Fe–Co nanowires with centered-staggered square structure, the especial stabilities are found at $x = 0.2, 0.6$, and 0.9 , and the binding energy at $x = 0.9$ is maximum.

From the fully relaxed structures of $\text{Fe}_{(1-x)}\text{Co}_x$ nanowires, we found the variation of wire lengths along the z-axis is negligible with the Co concentration. We compared the calculated lattice constants of Fe–Co nanowires with experimental results¹¹ (Figure 3). The calculated lattice constants of Fe–Co nanowires with centered-staggered square structure are slightly longer than experimental values. The experimental lattice constants rapidly decrease at $x = 0.2$ and slowly increase with increasing Co concentration,¹¹ while the calculated values for bcc Fe–Co bulks gradually go down from $x = 0.2$.¹⁵ We found that there is a common feature that the lattice constants of Fe-rich Fe–Co nanowires are longer than those of Co-rich nanowires. Actually the X-ray diffraction (XRD) spectrometer patterns show the structures of Fe–Co NCWs change from the bcc structure of Fe nanoclusters to the face-centered cubic (fcc) structure of Co nanoclusters,¹¹ like the FeCo binary nanoclusters and the bulk alloy. However, the structures of our Fe–Co nanowires maintain centered-staggered square for all Co concentrations, which is similar to the bcc structure. The

(11) Lee, G. H.; Huh, S. H.; Jeong, J. W.; Kim, S. H.; Choi, B. J.; Ri, H. C.; Kim, B.; Park, J. H. *J. Appl. Phys.* **2003**, *94*, 4179.

(12) Kresse, G.; Joubert, J. *Phys. Rev. B* **1999**, *59*, 1758.

(13) Jo, C.; Lee, J. I. *Phys. Status Solidi B* **2004**, *241*, 1427.

(14) Ziese, M.; Thornton, M. J., Ed.; *Spin Electronics*; Springer: New York, 2001.

(15) Pearson, W. B. *A Handbook of Lattice Spacings and Structure of Metals and Alloys*; Pergamon Press: New York, 1958.

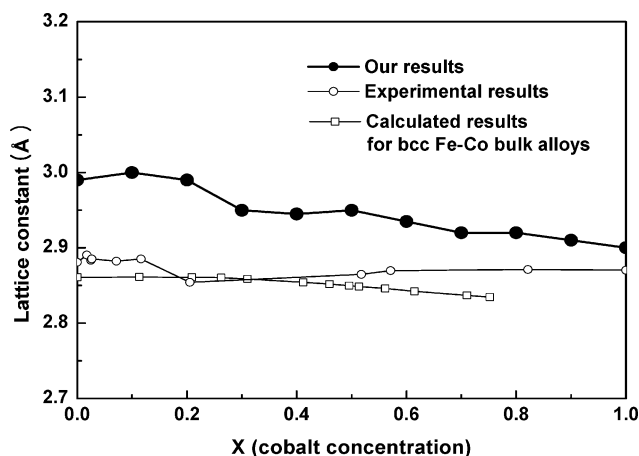


Figure 3. The lattice constants of $\text{Fe}_{(1-x)}\text{Co}_x$ nanowires with centered-staggered square structure (filled circle). The experimental results of free-standing Fe–Co nanowires with bcc structure are shown by open circle¹¹ and the calculated values for bcc Fe–Co bulk alloys at room temperature are indicated by open square.¹⁵

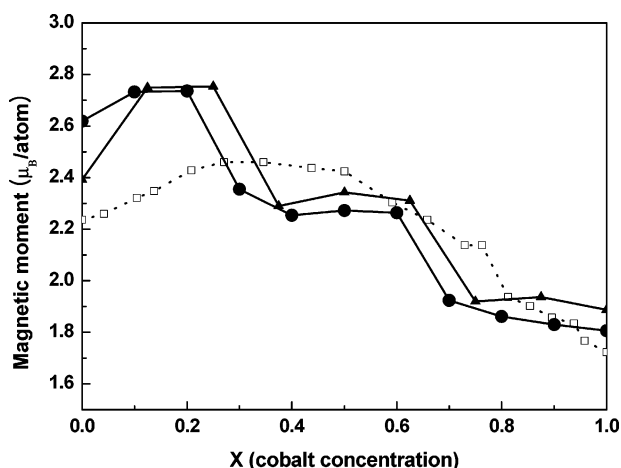


Figure 4. The calculated magnetic moments of $\text{Fe}_{(1-x)}\text{Co}_x$ nanowires with centered-staggered triangle (filled triangle) and square structure (filled circle). Open square denotes the Slater-Pauling curve.¹⁶

calculated lattice constants of Fe–Co nanowires with centered-staggered triangle structure have 3.38 Å for all Co concentrations, which shows the centered-staggered triangle structure is unfavorable for Fe–Co nanowires.

We have obtained the magnetic moments of Fe–Co nanowires with centered-staggered triangle and square structures (Figure 4). For Fe–Co nanowire with centered-staggered square structure, the highest magnetic moment appears near $x = 0.2$ and gradually decreases with increasing Co concentration. We find that the magnetic moments of $\text{Fe}_{(1-x)}\text{Co}_x$ nanowires in the range of $x = 0.1$ – 0.2 are $2.75 \mu_B/\text{atom}$, which is $0.35 \mu_B/\text{atom}$ larger than the highest magnetic moment of Fe–Co bulk alloys. In general, the magnitude of the magnetic moment is affected by the geometrical elements such as coordination number and bond length. We found the trend of the calculated magnetic moments is similar to that of lattice constants. Thus, there are plateaus in the range from 0.3 to 0.6 and from 0.7 to 1.0 due to the monotonic variation of lattice constants for Co concentration. The Slater-Pauling curve for the Fe–Co bulk alloys presents a peak near $x = 0.35$ and rapidly drops down at $x = 0.8$ where the Fe–Co bulk alloys change from bcc to fcc structure.¹⁶ Experiment also found that the structures of

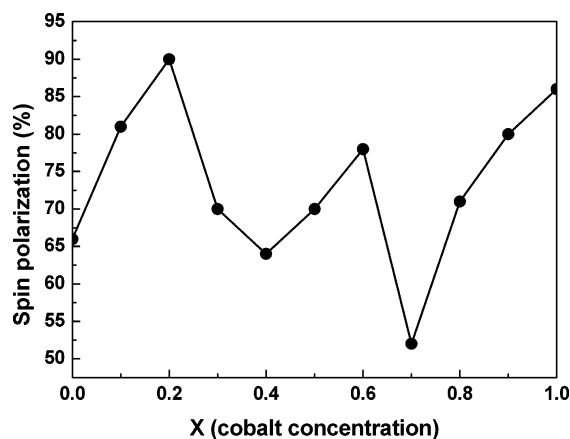


Figure 5. Spin polarization of free-standing $\text{Fe}_{(1-x)}\text{Co}_x$ nanowires with centered-staggered square structure.

Fe–Co nanowires change from bcc to fcc for high Co concentration.¹¹ The structures of nanowires geometrically depend on the central atoms in the Fe–Co nanowires (Figure 1). We found the magnetic moment of centered-staggered square Fe–Co nanowire is about 20% larger than that of staggered square nanowires without the central atoms. The central atoms are thus considered to play an important role in the structural change and the increase of the magnetic moment for Fe–Co nanowires. For the Fe–Co nanowires with centered-staggered triangle and square structures, the whole trend of their magnetic moments is similar to that of Fe–Co bulk alloys. We see that the magnetic moments depend mainly on the Co concentration regardless of nanowire shape.

We found that the density of states (DOS) at Fermi level for majority spin decreases as the Co concentration increases, which induces the enhanced spin polarization. The enhancement of spin polarization is important for spin-dependent electronic transport. According to Julliere's model,¹⁷ the magnitude of tunneling magnetoresistance (TMR) ratio depends on spin polarization. The spin polarization is obtained through $P = (\rho_i - \rho_l)/(\rho_i + \rho_l)$, where ρ_l (ρ_i) represents the DOS of majority (minority) spin at Fermi level. The spin polarizations for Fe–Co nanowires are shown in Figure 5. The spin polarizations of pure Fe and Co nanowires are 66% and 86%, respectively, while bcc Fe bulk (64%) has higher spin polarization compared with the value of fcc Co bulk (59%) in our calculation. We find $\text{Fe}_{0.8}\text{Co}_{0.2}$ nanowire has the highest spin polarization of 90% and reveals a nearly half-metallic character.

The DOS of pure Fe and Co nanowires with centered-staggered square structure are shown in Figure 6a. We found that the majority spin d band of pure Co nanowire is entirely occupied. The pure Co nanowire is a strong ferromagnet like bulk Co. The spd-orbital partial density of states (PDOS) of $\text{Fe}_{0.5}\text{Co}_{0.5}$ nanowire are shown in Figure 6b. The d-orbital PDOS of majority spin is almost occupied, and the d-orbital PDOS of minority spin shifts upward by an exchange splitting of about 0.8 eV. On the other hand, the charge density isosurface of majority spin has almost sphere shape

(16) Barthélemy, A.; Fert, A.; Petroff, F. *Handbook of Ferromagnetic Materials*; North-Holland: Amsterdam, 1999.

(17) Julliere, M. *Phys. Lett.* **1975**, 54A, 225.

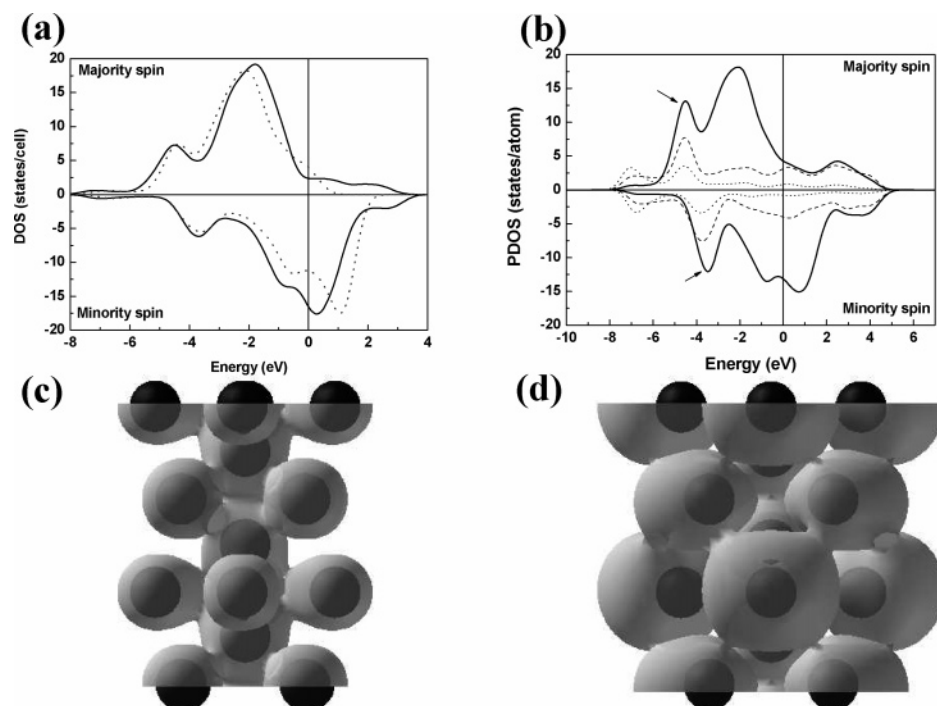


Figure 6. (a) The DOS of pure Co (solid line) and of pure Fe (dotted line) nanowire. (b) The d- (solid line), p- (dashed line), and s-orbital (dotted line) PDOS of Fe_{0.5}Co_{0.5} nanowire. The arrows indicate the PDOS peaks of the central atoms. The bonding charge density isosurface for (c) majority and (d) minority spin is formed at 0.413 and 0.006 e/Å³, respectively.

and a bonding is created along a nearest-neighbor distance of 2.31 Å at the charge density of 0.413 e/Å³ (Figure 6c). For minority spin, a bonding is formed on a wire length of 2.13 Å at the charge density of 0.006 e/Å³ with the oval shape of isosurface (Figure 6d).

The chain-of-spheres model can be used to understand the magnetization reversal process for magnetic nanowires, which is considered to be a chain of single-domain spheres with uniaxial magnetic anisotropy.⁴ In this model, the spheres are assumed to have no crystal anisotropy, and the shape anisotropy of the chains is obtained from the arrangement of the dipolar spheres. There are two reversal mechanisms for the chain of spheres, which are simultaneous parallel rotation of each of the dipole moments in the chain and symmetric fanning mechanism. To obtain the coercivity for Fe_(1-x)Co_x nanowires, one has to determine the aspect ratio n (length/area) of the nanowire. Zhan et al. used the aspect ratio of $n \approx 375$ for nanowire fabricated in porous anodic alumina templates.⁴ We set a slightly larger value ($n = 400$). Figure 7 shows the calculated coercivity of Fe_(1-x)Co_x nanowires using the chain-of-spheres model with a symmetric fanning magnetization reversal mechanism. The trend of coercivity obtained by the symmetric fanning mechanism agrees well with the experimental results for nanowire arrays inserted in porous templates. We find the free-standing Fe–Co nanowires have high coercivity of about 2500 Oe which is similar to the value of nanowire arrays combined in porous templates.

Conclusions

The possible structures of free-standing Fe–Co nanowires, their electronic structure, and magnetic properties are investigated by DFT calculations. The magnetic moments

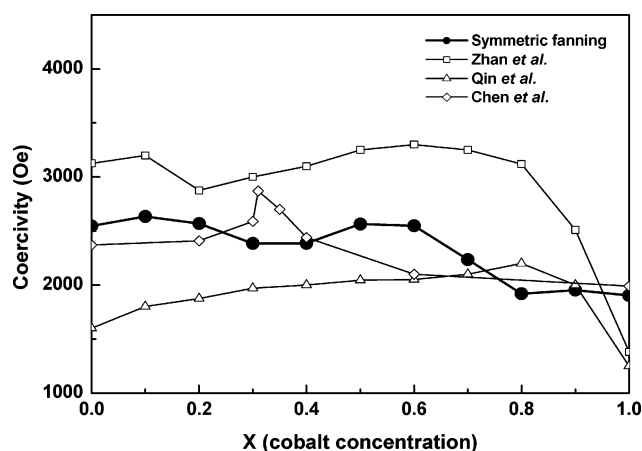


Figure 7. The calculated coercivity of Fe_(1-x)Co_x nanowires as a function of Co concentration using the chains-of-spheres model in the symmetric fanning (filled circle) mechanism. The values of calculated coercivity are compared with experimental results of Zhan et al.,⁴ Qin et al.,⁶ and Chen et al.⁷

of Fe-rich Fe–Co nanowires are higher than those of Fe–Co bulk alloys. The variation of magnetic moments are mainly dependent on the Co concentration regardless of nanowire shape, and the trend is similar to the lattice constants variation. The calculated lattice constants for Fe–Co nanowires with centered-staggered square structure are consistent with the experimental results for the free-standing Fe–Co nanowires. The pure Co nanowire has relatively large spin polarization, and the spin polarization of Fe_(1-x)Co_x at $x = 0.2$ is close to the half-metallic case. The values of calculated coercivity are as high as experimental results for Fe–Co nanowire arrays fabricated in porous templates. Our results suggest that free-standing Fe–Co nanowires with ferromagnetic character and high coercivity are promising candidates for spin-dependent

nanodevice and high-density magnetic recording media.

Acknowledgment. This work was supported by the Korea Science and Engineering Foundation (KOSEF) through the

electron Spin Science Center (eSSC) at Pohang University of Science and Technology (POSTECH).

CM047921J